

Measurement of Higgs couplings and mass in e^+e^- collisions at CLIC in the \sqrt{s} range of 350 GeV - 3 TeV

Tomáš Laštovička

Institute of Physics, Academy of Sciences, Prague

E-mail: lastovic@fzu.cz

on behalf of The CLIC Detector and Physics Study (CLICdp)

A future linear e^+e^- collider running at center-of-mass energies in the range from 350 GeV to 3 TeV provides excellent possibilities for Higgs precision measurements. Precision Higgs (and top) measurements can be performed around 350 GeV, where the Higgs is studied in a model-independent way through its recoil against a Z boson in the Higgs-strahlung process, providing not only an accurate mass measurement but also direct measurements of the branching ratios for most boson and fermion decay modes, including possible decays to invisible particles. At higher energies, the Higgs boson coupling to top quarks and the Higgs self-coupling can also be measured. For CLIC, these are studied at 1.4 TeV in Higgs production through WW fusion. At even higher energies, the rising WW fusion cross section, together with the higher machine luminosity, allows for the measurement of very small branching ratios. At the ultimate CLIC energy of 3 TeV this provides good precision for the Higgs coupling to muons and a currently unchallenged precision at the 10% level for the Higgs self-coupling. The prospects for these measurements at CLIC are based on detailed detector simulation studies including overlay of background from other physics processes and beam-induced backgrounds.

The European Physical Society Conference on High Energy Physics -EPS-HEP2013

18-24 July 2013

Stockholm, Sweden

1. Introduction

The Compact Linear Collider (CLIC) is an e^+e^- collider under development [1, 2, 3]. A novel two-beam acceleration technique is capable of providing accelerating gradients at the level of 100 MVm^{-1} . A staged approach for CLIC offers a unique physics program spanning over a number of decades. The first stage, at the $\sqrt{s} = 350 \text{ GeV}$ top quark production threshold, gives access to precision Higgs physics through Higgs-strahlung and WW fusion production processes. Such precision measurements will provide absolute values of Higgs couplings to fermions and bosons. The second stage, at 1.4 TeV , allows for the discovery of New Physics phenomena and gives access to additional Higgs properties, such as the top-Yukawa coupling, the Higgs potential and rare Higgs branching ratios. At the ultimate third stage CLIC energy of 3 TeV , the complete scope for precision Standard Model (SM) physics can be covered through precision measurements complemented by extended sensitivity to New Physics.

The detectors for the CLIC physics and detector studies [2] are based on the ILD and SiD detector concepts for the International Linear Collider (ILC). These concepts were optimised for the 3 TeV stage. The performance requirements are

- jet energy resolution of $\sigma_E/E \lesssim 3.5\%$ for jet energies from 100 GeV to 1 TeV ;
- track transversal momentum resolution of $\sigma_{p_T}/p_T^2 \lesssim 2 \cdot 10^{-5} \text{ GeV}^{-1}$;
- impact parameter resolution of $\sigma_{d_0}^2 = (5 \mu\text{m})^2 + (15 \mu\text{m})^2/p^2 \sin^3 \theta$;
- lepton identification efficiency better than 95% over the full range of energies;
- detector coverage for electrons down to very low polar angles θ .

The jet energy resolution is the main requirement that drives the detector design and optimisation. Consequently, both detector concepts are based on fine-grained calorimeters optimized for particle flow algorithms (PFAs), where all visible particles are reconstructed by combining information from precise tracking with calorimetry. The tracking detectors of CLIC_SiD are entirely based on silicon pixel and strip detectors, while CLIC_ILD tracker combines silicon pixels with silicon strips and a large Time Projection Chamber (TPC).

Bunch trains will arrive at the detector with a 50 Hz rate, each containing 312 bunch crossings at 0.5 ns time separation. Such a bunch separation allows for a power-pulsing scheme of the on-detector electronics, therefore reducing power consumption by a large factor. Less than one e^+e^- physics event is expected per bunch train. However, due to intense beamstrahlung, a high rate of incoherent e^+e^- pairs and of $\gamma\gamma \rightarrow \text{hadrons}$ events is expected. The beam-induced background will be significantly suppressed through precise hit timing (10 ns time-stamping for all silicon tracking elements and 100 ns precision on calorimeter hits) combined with offline event reconstruction with PFA. With properly selected cuts to eliminate reconstructed low- p_T particles, the average background level at 3 TeV can be reduced from approximately 20 TeV per bunch train to about 100 GeV per reconstructed physics event. The remaining particles can be further rejected by applying hadron-collider type jet-reconstruction algorithms.

2. Higgs Production at CLIC

A number of different production processes, accessible at the various CLIC energy stages, will allow precise measurements of the properties of a 125 GeV Standard Model (SM) like Higgs. The

Table 1: The leading-order Higgs *unpolarized* cross sections for the Higgs-strahlung, WW-fusion, and ZZ-fusion processes for $m_H = 125$ GeV at the three center-of-mass energies discussed in this document. The quoted cross sections include the effects of ISR but do not include the effects of beamstrahlung. Also listed are the numbers of expected events *including* the effects of beamstrahlung and ISR.

	350 GeV	1.4 TeV	3 TeV
\mathcal{L}_{int}	500 fb^{-1}	1500 fb^{-1}	2000 fb^{-1}
$\sigma(e^+e^- \rightarrow ZH)$	134 fb	9 fb	2 fb
$\sigma(e^+e^- \rightarrow H\nu_e\bar{\nu}_e)$	52 fb	279 fb	479 fb
$\sigma(e^+e^- \rightarrow H e^+e^-)$	7 fb	28 fb	49 fb
# ZH events	68,000	20,000	11,000
# $H\nu_e\bar{\nu}_e$ events	26,000	370,000	830,000
# $H e^+e^-$ events	3,700	37,000	84,000

processes with the highest cross section are shown in Figure 1. The expected number of ZH and $H\nu_e\bar{\nu}_e$ events at the different stages in a CLIC energy staged scenario is compared in Table 1 [4].

The results of the presented studies are based on detailed GEANT4 detector simulations, with the dominant $\gamma\gamma \rightarrow$ hadrons background overlaid and with full reconstruction of simulated events. All relevant SM background processes are considered.

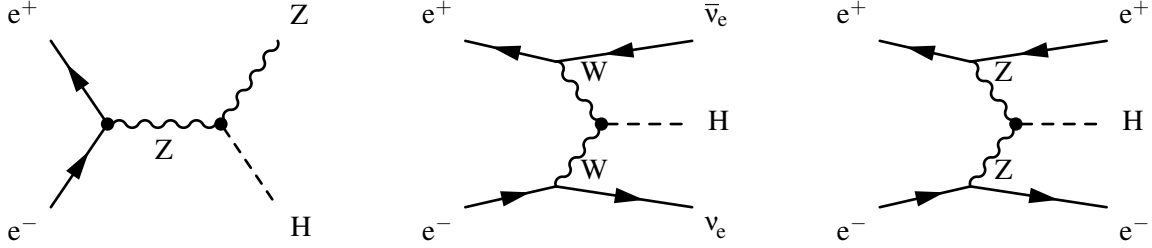


Figure 1: The three Higgs production processes at CLIC with the highest cross section. From left to right: Higgs-strahlung process (dominates below $\sqrt{s} \approx 500$ GeV), W-boson fusion and Z-boson fusion.

In addition to high cross section processes, an access is provided to top Yukawa coupling and trilinear Higgs self-coupling through the $e^+e^- \rightarrow t\bar{t}H$ and $e^+e^- \rightarrow HH\nu_e\bar{\nu}_e$ processes, shown in Figure 2.

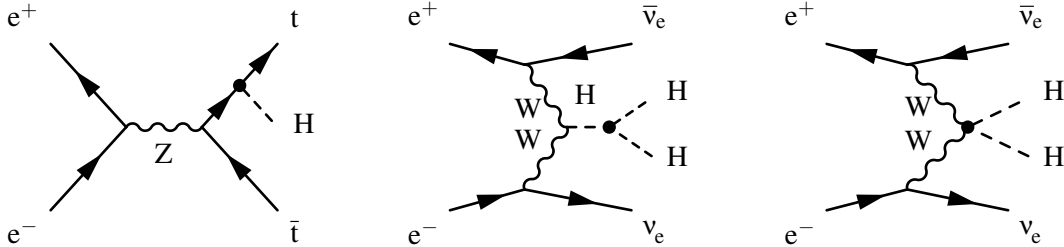


Figure 2: Rare processes at CLIC involving, from left to right, the top Yukawa coupling g_{tH} , the Higgs boson trilinear self-coupling λ and the quartic coupling g_{HHWW} .

All CLIC Higgs physics studies, presented in this paper, were performed assuming unpolarized e^+ and e^- beams. However, the CLIC baseline assumes electron polarization of $\pm 80\%$ with an option of positron polarisation at a lower level. Therefore, t-channel (WW fusion) and s-channel (Higgs-strahlung) processes can be enhanced by beam polarization and significant improvements in precision can be obtained. For example, assuming -80% polarisation of electrons, the cross section enhancement factor for WW-fusion is 1.80.

3. Measurements at 350 GeV

The Higgs-strahlung process offers a unique opportunity to study the Higgs coupling in a model independent way. This feature is unique to electron-positron colliders. The Higgs-strahlung events, from the $e^+e^- \rightarrow ZH$ process, may be identified solely from two oppositely charged leptons consistent with m_Z . Higgs decay particles are ignored in the event selection. Figure 3 shows a distribution of the invariant mass of the system recoiling against $Z \rightarrow \mu^+\mu^-$. A clear peak, corresponding to 125 GeV Higgs, is observed. This method provides an absolute measurement of the Higgs-strahlung cross section, independent of the Higgs boson decay modes, including invisible states.

The measurement of the absolute coupling of the Higgs boson to the Z boson can be obtained from the recoil mass distribution and plays a key role in the determination of absolute values of Higgs couplings at a linear collider. The precision can be further improved by using also the hadronic decay modes of the Z boson. For unpolarized beams, the study of simulated ZH recoil mass distributions for Z decaying into electrons and muons at CLIC operating at $\sqrt{s} = 350$ GeV, gives a statistical accuracy on the Higgs-strahlung cross section of approximately 4% for $m_H = 125$ GeV. The systematic uncertainty is expected to be significantly smaller.

The Higgs boson mass can be determined to a statistical precision of 120 MeV from the Z recoil mass distribution shown in Figure 3. This measurement can be further improved, to a precision better than 100 MeV, by employing the direct reconstruction of the decay products.

Subsequently, by identifying Higgs boson decay modes, measurements of the Higgs branching fractions can be made. Due to efficient flavour-tagging achievable at CLIC, the $H \rightarrow b\bar{b}$ and $H \rightarrow c\bar{c}$ channels can be separated. It is also possible to access the $H \rightarrow gg$ branching ratio. The results, including Higgs decays to τ , W and Z, are summarised in Table 2 [4].

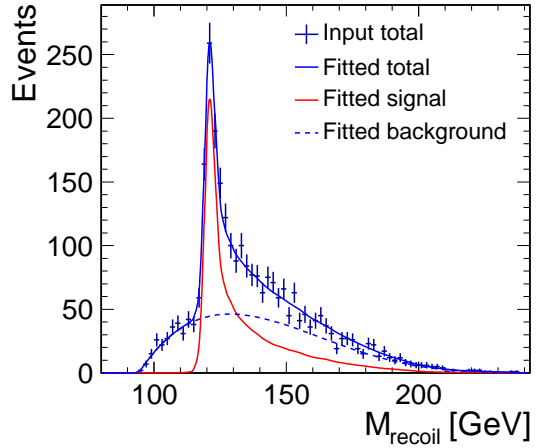


Figure 3: The distribution of Higgs recoil mass for $e^+e^- \rightarrow ZH \rightarrow \mu^+\mu^-H$ events with $m_H = 125$ GeV at $\sqrt{s} = 350$ GeV. The number of events is normalised to 500 fb^{-1} .

4. Measurements above 1 TeV

Above centre of mass energy of 1 TeV, both WW and ZZ fusion processes could deliver large samples of Higgs events. Relative couplings of the Higgs boson to the W and Z bosons can then be measured at the 1% level, therefore providing an important test of the SM prediction for $g_{HWW}/g_{HZZ} = \cos^2 \theta_W$, where θ_W is the weak mixing angle.

A clean jet flavour tagging along with high statistics samples of WW fusion events allows to determine the production rate of $e^+e^- \rightarrow H\nu_e\bar{\nu}_e \rightarrow b\bar{b}\nu_e\bar{\nu}_e$ to a statistical precision at the sub-% level. The Higgs production cross section, multiplied by a proper Higgs branching ratio, can be measured very precisely for a number of channels, see Table 2. The uncertainty of *relative* values of Higgs branching ratios will benefit from high statistics of Higgs events. For instance, at 3 TeV a statistical precision of 1.5 % can be reached on the ratio g_{Hcc}/g_{Hbb} . The uncertainty of *absolute* values of branching ratios can be determined in a combination with $\sqrt{s} = 350$ GeV Higgs-strahlung measurements. In addition, the large samples of $H \rightarrow b\bar{b}$ decays would allow the Higgs mass to be determined with a statistical precision of about 40 MeV and 33 MeV at 1.4 TeV and 3 TeV, respectively. Finally, it has been shown that the top Yukawa coupling can be measured with a precision of 4%.

See Table 2 for a summary of measurements at $\sqrt{s} = 1.4$ TeV and $\sqrt{s} = 3$ TeV.

5. Higgs boson trilinear self-coupling

The measurement of the Higgs self-coupling strength provides a direct access to the Higgs potential, namely to the quartic potential coupling λ . This measurement is an essential part of a quest to establish the Higgs mechanism experimentally. Such an experiment is extremely challenging at the LHC, even with 3000 fb^{-1} of data. Even at a linear collider with \sqrt{s} above 1 TeV a large integrated luminosity is required. The most favourable channel for this measurement is the $e^+e^- \rightarrow HH\nu_e\bar{\nu}_e$, see Figure 2. The uncertainty of λ is evaluated by measuring the uncertainty of this process and relating it to that of λ via a conversion factor. An alternative approach employs template fitting of the neural net classifier output distribution [5], employed to select signal events, in order to obtain the uncertainty on λ directly. Results from a detailed study estimate that a precision of 28% and 16% on λ can be achieved at CLIC operating respectively at $\sqrt{s} = 1.4$ TeV and $\sqrt{s} = 3$ TeV, see Table 2. With 80% electron beam polarization and 30% positron beam polarization a measurement precision at the 10% level can be reached at CLIC operating at $\sqrt{s} = 3$ TeV.

In an alternative way, the analysis of the same process can be interpreted as fully due to the quartic coupling g_{HHWW} , see Figure 2. A preliminary study suggests that a measurement precision of 7% and 3% on g_{HHWW} can be achieved at CLIC operating at $\sqrt{s} = 1.4$ TeV and $\sqrt{s} = 3$ TeV, respectively.

References

- [1] M. Aicheler *et al.* (editors), *A Multi-TeV Linear Collider based on CLIC Technology: CLIC Conceptual Design Report*, CERN-2012-007, JAI-2012-001, KEK Report 2012-1, PSI-12-01, SLAC-R-985 [<https://edms.cern.ch/document/1234244>].

Table 2: The precisions obtainable for the Higgs observables at CLIC for integrated luminosities of 500 fb^{-1} at $\sqrt{s} = 350 \text{ GeV}$, 1.5 ab^{-1} at $\sqrt{s} = 1.4 \text{ TeV}$, and 2.0 ab^{-1} at $\sqrt{s} = 3.0 \text{ TeV}$. In all cases, except the last, unpolarized beams have been assumed. The majority of the results are from the full detector simulation and reconstruction including overlaid background from $\gamma\gamma \rightarrow \text{hadrons}$. The numbers marked by ‘*’ are preliminary and the numbers marked by ‘†’ are estimates. The ‘–’ indicates that a measurement is not possible or relevant at this center-of-mass energy and ‘tbd’ indicates that no results or estimates are yet available. For the branching ratios, the measurement precision refers to the expected statistical uncertainty on the product of the relevant cross section and branching ratio; this is *equivalent* to the expected statistical uncertainty of the product of couplings and Γ_H . For the measurements from the $t\bar{t}H$ and $HH\nu_e\bar{\nu}_e$ processes, the measurement precisions give the expected statistical uncertainties on the quantity or quantities listed under the observable heading.

Channel	Measurement	Observable	Statistical precision		
			350 GeV 500 fb^{-1}	1.4 TeV 1.5 ab^{-1}	3.0 TeV 2.0 ab^{-1}
ZH	Recoil mass distribution	m_H	120 MeV	–	–
ZH	$\sigma(\text{HZ}) \times BR(\text{H} \rightarrow \text{invisible})$	Γ_{inv}	tbd	–	–
ZH	$\text{H} \rightarrow b\bar{b}$ mass distribution	m_H	tbd	–	–
$\text{H}\nu_e\bar{\nu}_e$	$\text{H} \rightarrow b\bar{b}$ mass distribution	m_H	–	40 MeV*	33 MeV*
ZH	$\sigma(\text{HZ}) \times BR(\text{Z} \rightarrow \ell^+\ell^-)$	g_{HZZ}^2	4.2%	–	–
ZH	$\sigma(\text{HZ}) \times BR(\text{H} \rightarrow b\bar{b})$	$g_{\text{HZZ}}^2 g_{\text{Hbb}}^2 / \Gamma_H$	1%†	–	–
ZH	$\sigma(\text{HZ}) \times BR(\text{H} \rightarrow c\bar{c})$	$g_{\text{HZZ}}^2 g_{\text{Hcc}}^2 / \Gamma_H$	5%†	–	–
ZH	$\sigma(\text{HZ}) \times BR(\text{H} \rightarrow g\bar{g})$		6%†	–	–
ZH	$\sigma(\text{HZ}) \times BR(\text{H} \rightarrow \tau^+\tau^-)$	$g_{\text{HZZ}}^2 g_{\text{H}\tau\tau}^2 / \Gamma_H$	5.7%	–	–
ZH	$\sigma(\text{HZ}) \times BR(\text{H} \rightarrow \text{WW}^*)$	$g_{\text{HZZ}}^2 g_{\text{HWW}}^2 / \Gamma_H$	2%†	–	–
ZH	$\sigma(\text{HZ}) \times BR(\text{H} \rightarrow \text{ZZ}^*)$	$g_{\text{HZZ}}^2 g_{\text{HZZ}}^2 / \Gamma_H$	tbd	–	–
$\text{H}\nu_e\bar{\nu}_e$	$\sigma(\text{H}\nu_e\bar{\nu}_e) \times BR(\text{H} \rightarrow b\bar{b})$	$g_{\text{HWW}}^2 g_{\text{Hbb}}^2 / \Gamma_H$	3%†	0.3%	0.2%
$\text{H}\nu_e\bar{\nu}_e$	$\sigma(\text{H}\nu_e\bar{\nu}_e) \times BR(\text{H} \rightarrow c\bar{c})$	$g_{\text{HWW}}^2 g_{\text{Hcc}}^2 / \Gamma_H$	–	2.9%	2.7%
$\text{H}\nu_e\bar{\nu}_e$	$\sigma(\text{H}\nu_e\bar{\nu}_e) \times BR(\text{H} \rightarrow g\bar{g})$		–	1.8%	1.8%
$\text{H}\nu_e\bar{\nu}_e$	$\sigma(\text{H}\nu_e\bar{\nu}_e) \times BR(\text{H} \rightarrow \tau^+\tau^-)$	$g_{\text{HWW}}^2 g_{\text{H}\tau\tau}^2 / \Gamma_H$	–	3.7%	tbd
$\text{H}\nu_e\bar{\nu}_e$	$\sigma(\text{H}\nu_e\bar{\nu}_e) \times BR(\text{H} \rightarrow \mu^+\mu^-)$	$g_{\text{HWW}}^2 g_{\text{H}\mu\mu}^2 / \Gamma_H$	–	29%*	16%
$\text{H}\nu_e\bar{\nu}_e$	$\sigma(\text{H}\nu_e\bar{\nu}_e) \times BR(\text{H} \rightarrow \gamma\gamma)$		–	15%*	tbd
$\text{H}\nu_e\bar{\nu}_e$	$\sigma(\text{H}\nu_e\bar{\nu}_e) \times BR(\text{H} \rightarrow \text{Z}\gamma)$		–	tbd	tbd
$\text{H}\nu_e\bar{\nu}_e$	$\sigma(\text{H}\nu_e\bar{\nu}_e) \times BR(\text{H} \rightarrow \text{WW}^*)$	$g_{\text{HWW}}^4 / \Gamma_H$	tbd	1.1%*	0.8%*
$\text{H}\nu_e\bar{\nu}_e$	$\sigma(\text{H}\nu_e\bar{\nu}_e) \times BR(\text{H} \rightarrow \text{ZZ}^*)$	$g_{\text{HWW}}^2 g_{\text{HZZ}}^2 / \Gamma_H$	–	3%†	2%†
$\text{H}e^+e^-$	$\sigma(\text{H}e^+e^-) \times BR(\text{H} \rightarrow b\bar{b})$	$g_{\text{HZZ}}^2 g_{\text{Hbb}}^2 / \Gamma_H$	–	1%†	0.7%†
$t\bar{t}H$	$\sigma(t\bar{t}H) \times BR(\text{H} \rightarrow b\bar{b})$	$g_{\text{H}t\bar{t}}^2 g_{\text{Hbb}}^2 / \Gamma_H$	–	8%	tbd
$HH\nu_e\bar{\nu}_e$	$\sigma(HH\nu_e\bar{\nu}_e)$	g_{HHWW}	–	7%*	3%*
$HH\nu_e\bar{\nu}_e$	$\sigma(HH\nu_e\bar{\nu}_e)$	λ	–	28%	16%
$HH\nu_e\bar{\nu}_e$	with -80% e^- polarization	λ	–	21%	12%

- [2] L. Linssen *et al.* (editors), *Physics and Detectors at CLIC: CLIC Conceptual Design Report*, ANL-HEP-TR-12-01, CERN-2012-003, DESY 12-008, KEK Report 2011-7 [arXiv:1202.5940].
- [3] P. Lebrun *et al.* (editors), *The CLIC Programme: towards a staged e^+e^- Linear Collider exploring the Terascale*, ANL-HEP-TR-12-51, CERN-2012-005, KEK Report 2012-2, MPP-2012-115 [<https://edms.cern.ch/document/1234246>].
- [4] H. Abramowicz *et al.* [CLIC Detector and Physics Study Collaboration], *Physics at the CLIC e^+e^- Linear Collider - Input to the Snowmass process 2013* [arXiv:1307.5288].
- [5] T. Laštovička and J. Strube, *Measurement of the trilinear Higgs coupling at 1.4 TeV and 3 TeV CLIC*, LCD-Note-2012-014, in preparation.